Kinetic Evidence for Peptide-Induced Oligomerization of the Molecular Chaperone DnaK at Heat Shock Temperatures†

Carol D. Farr and Stephan N. Witt*

Department of Biochemistry and Molecular Biology, Louisiana State University Medical Center, 1501 Kings Highway, Shreveport, Louisiana 71130-3932

Received May 8, 1997; Revised Manuscript Received July 1, 1997⊗

ABSTRACT: The pre-steady-state kinetics of the binding of a fluorescent peptide (dansyl-KLIGVLSSLFRPK, fVSV13) to the *Escherichia coli* molecular chaperone DnaK were investigated over a range of temperatures (25−42 °C). At 42 °C, over a wide range of peptide concentrations, the fVSV13 peptide bound to DnaK with biphasic kinetics: a rapid burst in the DnaK−fVSV13 signal in the first 5 s was followed by a gradual reduction in the signal over the next 100 s. The descending portion of each biphasic trace followed the equation $F(t) = \Delta F \exp(-k_d t) + F_\infty$, where ΔF, k_d, and F_∞ are the amplitude, the apparent first-order rate constant, and the fluorescence end point, respectively. Both ΔF and k_d increased with increasing concentrations of DnaK, which suggests that the loss of the DnaK−fVSV13 signal is caused by a bimolecular reaction. We propose that (i) the fVSV13 peptide binds to and induces a conformational change in the DnaK monomer [E + P ⇌ (EP)*]; and (ii) the conformational change promotes the formation of oligomeric DnaK−peptide complexes [E_n + (EP)* ⇌ E_n−EP]. The term (EP)* denotes a monomeric DnaK−peptide complex in which the bound peptide is fluorescent; E_n−EP denotes an oligomeric DnaK−peptide complex in which the fluorescence of the bound peptide is quenched. Numerical fitting of the stopped-flow data to reactions (i) and (ii) yielded values for the four rate constants. When the proposed kinetic model was tested by conducting experiments in the presence of excess peptide or excess ATP—conditions which inhibit oligomerization—DnaK−fVSV13 complex formation proceeded to stable asymptotes, with no reduction in the DnaK−fVSV13 signal at long times.

Molecular chaperones of the 70-kDa family, both stress induced (Hsp70)[1] and constitutively-expressed (Hsc70), utilize free energy from ATP binding and hydrolysis to selectively bind and release segments of partially unfolded proteins. This cycle of substrate binding and release, which is coupled to conformational changes in the chaperone, promotes a variety of protein−protein interactions, such as the stabilization of nascent and partially unfolded proteins, the translocation of substrate proteins, and the assembly and disassembly of protein complexes [for reviews, see Georgopoulos and Welch (1993), Hendrick and Hartl (1993), and Becker and Craig (1994)]. The molecular mechanism that enables a single chaperone molecule to interact with many different target sequences is the subject of intense investigation.

Molecular chaperones (70 kDa) consist of two functional domains. ATP binding and hydrolysis occur in the NH_2-terminal domain, and selective substrate binding and release occur in the COOH-terminal domain. While the three-dimensional structure of a 70-kDa molecular chaperone is not known, the structures of the separate functional domains have been determined. The NH_2-terminal domain of Hsc70, similar to the structure of both hexokinase and actin (Flaherty et al., 1990, 1991), contains two lobes that are separated by a cleft in which the nucleotide binds. The COOH-terminal domain of the *Escherichia coli* Hsp70 DnaK (residues 389−607) contains a β-sandwich subdomain that is topped by α-helical segments; the peptide binds in a channel formed by loops from the β-sandwich (Zhu et al., 1996). Several biophysical studies have shown that Mg-ATP binding to the ATPase domain induces a global conformational change in the chaperone, yielding a state which has reduced affinity for (poly)peptides (Palleros et al., 1993b; Ha & McKay, 1995; Shi et al., 1996). Conversely, since peptide binding to the substrate-binding domain stimulates ATP hydrolysis (Flynn et al., 1989; Sadis & Hightower, 1992; Blond-Elguindi et al., 1993; Benaroudj et al., 1994; Fourie et al., 1994; Farr et al., 1995), peptide binding must also alter the conformation of the chaperone (Fung et al., 1996).

In the course of investigating the effect of temperature on the kinetics of DnaK−fVSV13 complex formation and dissociation using stopped-flow fluorescence, we discovered that DnaK−fVSV13 complex formation is biphasic, especially at heat shock temperatures. The stopped-flow traces were characterized by a rapid burst in the DnaK−fVSV13 signal followed by a gradual reduction in the signal. In some cases, the reduction in the DnaK−fVSV13 signal was so great that the traces were almost "bell-shaped." In this report, experiments were designed to determine the molecular events which cause this reduction in fluorescence after the initial burst. It is important to understand the cause of the reduction

† Support for this work came from the National Institutes of Health (GM51521) and the American Cancer Society (JFRA-583).

* To whom correspondence should be addressed. Telephone: (318) 675-7891. FAX: (318) 675-5180. E-mail: SWITT1@MAIL.SH.LSUMC.EDU.

⊗ Abstract published in *Advance ACS Abstracts,* August 15, 1997.

[1] Abbreviations: HEPES, *N*-(2-hydroxyethyl)piperazine-*N*′-2-ethanesulfonic acid; Hsc70, 70-kDa heat shock cognate protein; Hsp70, 70-kDa heat shock protein; fVSV13, α-*N*-dansyl-peptide derived from residues 490−502 of the vesicular stomatitis virus (New Jersey serotype) glycoprotein (KLIGVLSSLFRPK); SDS−PAGE, sodium dodecyl sulfate−polyacrylamide gel electrophoresis.

S0006-2960(97)01082-9 CCC: $14.00

in the DnaK−fVSV13 signal so that peptide on- and off-rate constants can be accurately determined. Evidence is presented herein that the descending phase of the stopped-flow traces is a consequence of peptide-induced oligomerization of DnaK. An analysis of the effect of nucleotide on the activation energy barriers to DnaK−fVSV13 complex formation and dissociation will be given in a subsequent report (Farr and Witt, manuscript in preparation).

MATERIALS AND METHODS

Protein. All reagents were of the highest purity and were purchased from Sigma, unless stated otherwise. The *E. coli* strain RLM893 (Zylicz & Georgopoulos, 1984) was used to obtain DnaK. The protein was isolated as previously described (Farr et al., 1995) and stored in a HEPES sample buffer (25 mM HEPES/50 mM KCl/5 mM $MgCl_2$/5 mM 2-mercaptoethanol at pH 7.0). SDS−PAGE of purified DnaK revealed one band at 70 ± 1 kDa, and densitometric scans of the gel show that the protein is >95% pure. Protein concentration was determined by the BioRad protein assay according to the manufacturer's instructions and verified by an absorbance determination using the extinction coefficient $\epsilon_{280} = 15.8 \times 10^3\ M^{-1}\ cm^{-1}$ (Montgomery et al., 1993). The amount of nucleotide in DnaK preparations was determined by the A_{280}/A_{260} ratio; in every case, $A_{280}/A_{260} > 1.5$, which indicates that the protein is nucleotide-free (Chaykin, 1966). No corrections were made for the slight variation of the pH of the HEPES sample buffer over the temperature range (25−42 °C) at which samples were incubated. For the stopped-flow experiments, DnaK was concentrated using Amicon microconcentrators (Centricon 30), and after the procedure, the concentration was redetermined using the Bio-Rad assay. The kinetic effect described in this report was reproduced in more than 10 different DnaK preparations.

Peptides. The VSV13 peptide, which represents amino acids 490−502 of the vesicular stomatitis virus (New Jersey serotype) glycoprotein (KLIGVLSSLFRPK) (Gallione & Rose, 1983), was purchased from the University of Kentucky Core Facility (Lexington, KY). The peptide was NH_2-terminally-labeled with the environmentally sensitive fluorophore dansyl chloride [5-(dimethylamino)naphthalene-1-sulfonyl chloride] as previously described (Farr et al., 1995). Unlabeled VSV13 was sequenced at the University of Kentucky, and the mass of the labeled VSV13 peptide, which is referred to as fVSV13, was verified using electrospray mass spectrometry at the Louisiana State University Core Facility (New Orleans, LA). The VSV13 peptide is also referred to as peptide C (Flynn et al., 1989).

Instrumentation. An Applied Photophysics Ltd. (Leatherhead, U.K.) stopped-flow spectrometer (SX-17MV) was used to follow the rapid reaction between DnaK and the fVSV13 peptide. The excitation wavelength ($\lambda_{ex} = 335$ nm) was selected using a monochromator. The excitation bandwidth was varied from 0.5 to 4.6 nm, depending on the fVSV13 concentration. A photomultiplier tube was attached at 90° to the incident light to collect fluorescence emission, and an Oriel long-pass filter with a cutoff wavelength of 399 nm was used to eliminate stray excitation radiation. The instrumental time constant was typically less than or equal to 1% of the time required to reach the maximum fluorescence intensity. Samples were degassed prior to loading into the stopped-flow syringes. One syringe contained fVSV13, the other DnaK. For the experiments conducted with nucleotide, the nucleotide was always added to the solution of DnaK. Thus, upon mixing, fVSV13 peptides bound to nucleotide-charged DnaK molecules. Concentrations of DnaK, fVSV13, and nucleotide within the text refer to concentrations after mixing. Temperature control of the reactants and the jacketed mixing chamber was achieved with a circulating external water bath ($T = \pm 0.1$ °C). Stopped-flow traces are the average of from 7 to 10 individual traces. In some cases, data were collected using a split time base mode.

Chemical Cross-Linking. The effect of DnaK concentration as well as nucleotide on oligomerization in the absence of peptide was determined using a chemical cross-linking assay (Schlossman et al., 1984; Hames & Rickwood, 1990). DnaK samples were incubated in 1.5 mL siliconized Eppendorf tubes for 10 min at the desired temperature either in the absence or in the presence of nucleotides. To cross-link, samples were incubated with glutaraldehyde for 1 min at 42 °C or 2 min at 25 °C, followed by the addition of 80 mM $NaBH_4$ (on ice for 10 min), 200 mM Tris-HCl, pH 7.4 (on ice for 5 min), and 10% trichloroacetic acid with 0.2% Triton X-100 (on ice for 30 min). The samples were centrifuged (14000*g* for 10 min), washed with ethanol/ether (1:1 v/v), and then centrifuged (14000*g* for 10 min). Final concentrations of the reactants during cross-linking were [DnaK] = 1−12 μM, [nucleotide] = 2 mM, and [glutaraldehyde] = 11 mM. The final volume of each sample was 220 μL.

Electrophoresis. Glutaraldehyde-treated DnaK samples were analyzed using SDS−PAGE (Laemmli, 1970). Sample pellets from the chemical cross-linking assay were dissolved in 50 μL of loading buffer (3% w/v SDS/10% v/v glycerol/0.008% w/v bromophenol blue/7% v/v 2-mercaptoethanol/62 mM Tris, pH 6.8) and boiled for 2 min prior to loading. Gels were stained with Coomassie Brilliant Blue G-250 and scanned with a Molecular Dynamics densitometer.

Analysis of the Descending Portion of the Stopped-Flow Traces. In many cases, the stopped-flow data were characterized by both an ascending portion and a descending portion. Such traces are referred to as "biphasic" DnaK−fVSV13 complex formation traces. The descending portions were fitted to the equation $F(t) = \Delta F \exp(-k_d t) + F_\infty$, where ΔF, k_d, and F_∞ are the amplitude, the apparent first-order rate constant, and the fluorescence end point, respectively, using a curve-fitting program supplied with the Applied Photophysics instrument. The program fit the stopped-flow data to the above exponential function using a Marquardt algorithm based on the program Curfit given in Bevington (1969). At each DnaK concentration, 7−10 stopped-flow traces were collected and analyzed to determine $k_d(T)$ values. The average $k_d(T)$ value was then plotted versus [DnaK]. The uncertainty in each average $k_d(T)$ value is given by the error bar, which represents twice the average deviation. To assess the reproducibility of the stopped-flow experiments, on separate days and using different preparations of DnaK, kinetic experiments were repeated for most DnaK concentrations; those average $k_d(T)$ values are also shown in the $k_d(T)$ vs [DnaK] plots.

Numerical Fitting. The program Scientist 2.0 (MicroMath, Salt Lake City, UT) was used for fitting stopped-flow data to the proposed kinetic mechanism. Scientist fits experi-

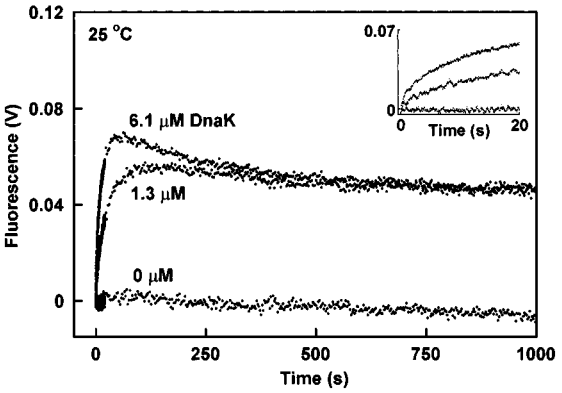

FIGURE 1: Pre-steady-state kinetics of fVSV13 binding to DnaK at 25 °C. The reaction between DnaK and fVSV13 was followed by stopped-flow fluorescence spectrophotometry. The inset shows DnaK−fVSV13 complex formation at early times. Data were collected in a split time-base mode: i.e., 400 points were collected in the first 20 s, and 400 points were collected in the last 1000 s. Conditions: [fVSV13] = 0.1 μM; [DnaK] = 0, 1.3, 6.1 μM; λ_{ex} = 335 nm (2.5 nm bandwidth). The signal F is in volts from a photomultiplier tube. There is a 15% variation in the voltage values.

mental data to a kinetic model by numerically integrating rate equations and then minimizing the sum of the squares of the residuals using a variant of the Levenberg−Marquardt method. The user specifies the rate equations, the initial concentrations of reactants, and the initial guesses for the rate constants.

RESULTS

Pre-Steady-State Kinetics of fVSV13 Binding to DnaK. The pre-steady-state kinetics of fVSV13 binding to DnaK were investigated at 25, 37, and 42 °C using stopped-flow fluorescence. The reaction was followed by monitoring the increase in fluorescence which accompanies the binding of this peptide to DnaK (Farr et al., 1995). The observed increase in fluorescence is referred to as the DnaK−fVSV13 signal. Most of the kinetic experiments were conducted by varying [DnaK] (1−7 μM) at a fixed concentration of fVSV13 (0.1 μM), while others were conducted by varying [fVSV13] (6−60 μM) at a fixed concentration of DnaK (6 μM).

At 25 °C, when the concentration of the fVSV13 peptide was about one-tenth the concentration of DnaK ([fVSV13]/[DnaK] = 0.1 μM/1.3 μM = 0.08), the increase in the DnaK−fVSV13 signal followed simple exponential kinetics over 1000 s (Figure 1). In contrast, when the concentration of the fVSV13 peptide was one-sixtieth that of DnaK ([fVSV13]/[DnaK] = 0.1 μM/6.1 μM = 0.02), DnaK−fVSV13 complex formation was biphasic. In this case, the DnaK−fVSV13 signal reached a maximum value at 60 s and then gradually decreased by 23% over 1000 s (ΔF = 0.016 V). The inset to Figure 1 shows that the initial rate of complex formation increased as the concentration of DnaK was increased from 1.3 to 6.1 μM. As shown below, the descending portion of the stopped-flow traces was even more pronounced when experiments were conducted at temperatures above 25 °C.

Figure 2A shows the effect of varying the DnaK concentration (1−7 μM) at a fixed concentration of fVSV13 (0.1 μM) in the absence of nucleotide at 42 °C. The family of traces exhibited the following features. (i) When [DnaK] = 1.1 μM, complex formation yielded a nearly stable asymptote. (ii) The time (t_{max}) to reach the fluorescence maximum (F_{max}) decreased as the concentration of DnaK was increased. At 3.2 and 5.6 μM DnaK, t_{max} = 18 and 7 s, respectively. (iii) Above approximately 3 μM DnaK, the value of the fluorescence end point at 200 s (F_∞) *decreased* as the concentration of DnaK was increased. At 3.2 and 5.6 μM DnaK, F_∞ = 0.022 and 0.007 V, respectively. (iv) The descending phase of each biphasic trace followed the equation $F(t) = \Delta F \exp(-k_d t) + F_\infty$, where ΔF, k_d, and F_∞ are the amplitude, the apparent first-order rate constant, and the fluorescence end point, respectively. The results show that ΔF (Figure 2A) and k_d (Figure 2B) both increased as the DnaK concentration was increased. Since the oligomerization of DnaK and other 70-kDa chaperones also increases in a concentration-dependent manner (Palleros et al., 1993a; Benaroudj et al., 1995; Schönfeld et al., 1995; Gao et al., 1996), we hypothesized that the reduction in the DnaK−fVSV13 signal in the biphasic traces was linked to DnaK oligomerization.

Effect of Nucleotide on the Pre-Steady-State Kinetics of fVSV13 Binding to DnaK. It is well-known that ATP inhibits chaperone oligomerization (Schmid et al., 1985; Carlino et al., 1992; Palleros et al., 1993a; Toledo et al., 1993; Benaroudj et al., 1994; Gao et al., 1996; Shi et al., 1996). Thus, if oligomerization was responsible for the reduction in the DnaK−fVSV13 signal in the biphasic traces, then ATP should abolish the reduction because it inhibits oligomerization. This idea was tested by conducting kinetic experiments in the presence of ATP. The effect of ADP was also assessed. These experiments were conducted by rapidly mixing fVSV13 with an equal volume of DnaK containing 2.0 mM nucleotide. Results are shown in Figures 2C,D.

Figure 2C shows stopped-flow traces obtained upon the rapid mixing of the fVSV13 peptide with DnaK and Mg-ATP. This family of traces exhibited the following features. As the concentration of DnaK was increased from 1 to 6 μM, both the initial rate of DnaK−fVSV13 complex formation (Figure 2C, inset) and the magnitude of the asymptote at 200 s increased (from 0.015 to 0.040 V), as expected. No reduction in the DnaK−fVSV13 signal was observed over the time course of the measurements (200 s). The results show that Mg-ATP prevents the reduction in the DnaK−fVSV13 signal.

Figure 2D shows stopped-flow traces obtained upon the rapid mixing of the fVSV13 peptide with DnaK and Mg-ADP. The family of traces exhibited similar features as those obtained in the absence of nucleotide (see above). The inset shows that the initial rate of complex formation increased with increasing concentrations of DnaK. Note that the DnaK−fVSV13 signal (F_{max}) with ADP was about twice that observed when no nucleotide was present; therefore, approximately twice as many DnaK−fVSV13 complexes formed in the presence of Mg-ADP as in its absence (compare Figure 2A and Figure 2D). Note that, at similar DnaK concentrations, the magnitudes (ΔF) of the descending portions of the stopped-flow traces in Figure 2A,D are similar. In both cases, the descending portion of the stopped-flow traces was more prominent as the DnaK concentration was increased.

The dependence of k_d on the concentration of DnaK was examined in detail over a range of temperatures (25−42 °C). Two composite plots of $k_d(T)$ versus [DnaK] are shown in Figure 2 (panels B and E). In both plots, k_d exhibited a linear

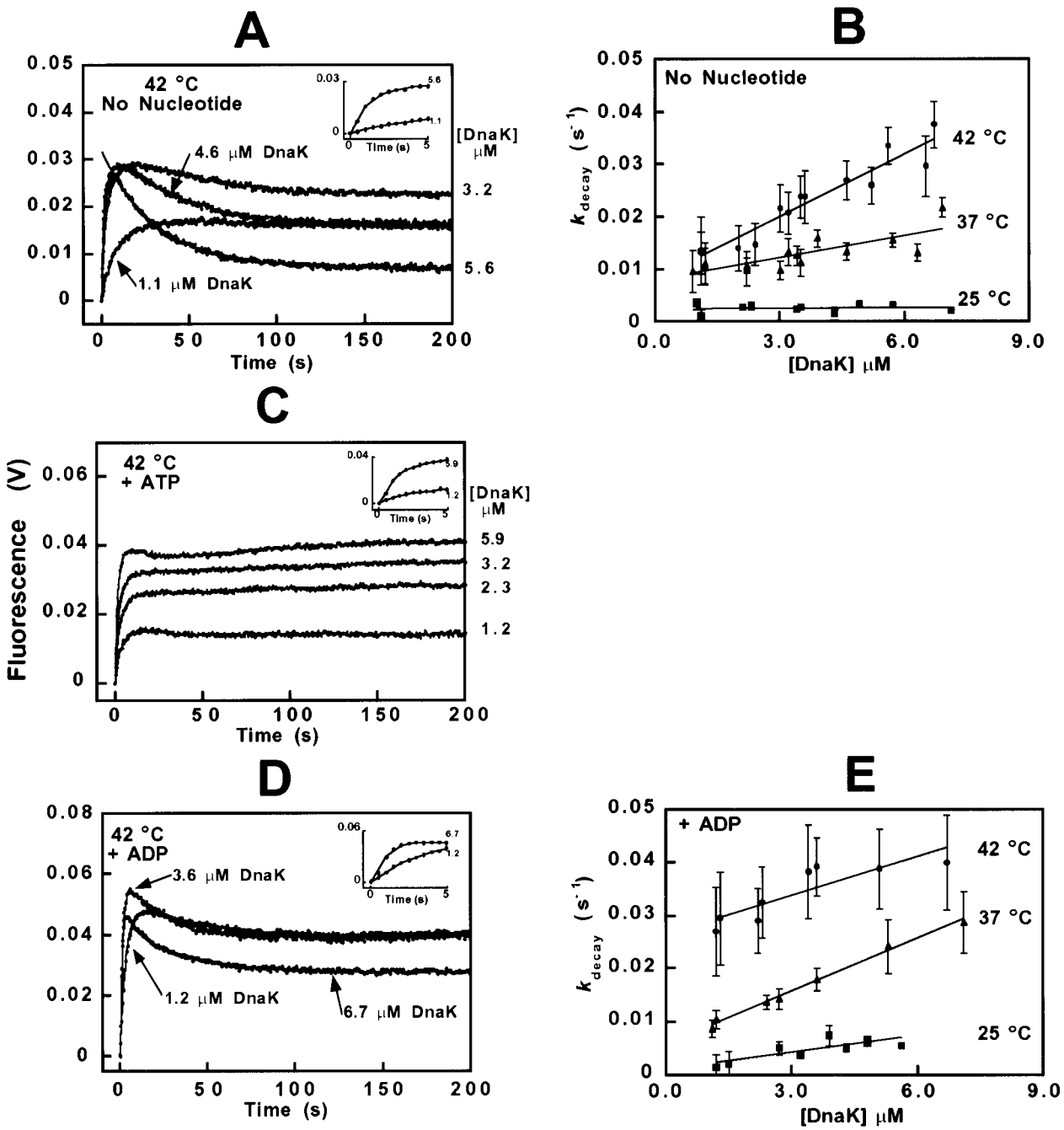

FIGURE 2: Effect of nucleotide on the pre-steady-state kinetics of DnaK−fVSV13 complex formation at 42 °C. The kinetic experiments were conducted by varying the concentration of DnaK (1.0−6.7 μM) at a fixed concentration of fVSV13 (0.1 μM). DnaK−fVSV13 complex formation at 42 °C is shown in panels A (no nucleotide), C (1.0 mM ATP), and D (1.0 mM ADP). (The insets show complex formation at early times.) The descending portion of each curve in panels A and D was fitted to the function $F(t) = \Delta F \exp(-k_d t) + F_\infty$. The best fit to the descending portion of the 5.6 μM DnaK trace in panel A is $F(t) = 0.0251 \exp(-0.033t) + 0.007$ (solid line). (Traces obtained at 25 and 37 °C were analyzed in the same way.) Plots of $k_d(T)$ versus [DnaK] are shown in panels B (no nucleotide) and E (+ADP). The slopes of the plots are 40 ± 130, 1400 ± 300, and 4000 ± 400 M^{-1} s^{-1}, respectively, at 25, 37, and 42 °C (B, no nucleotide); the slopes of the plots are 1100 ± 300, 3300 ± 130, and 2400 ± 600 M^{-1} s^{-1}, respectively, at 25, 37, and 42 °C (E, +ADP). Conditions: λ_{ex} = 335 nm (5 nm bandwidth); temperature = 25, 37, and 42 °C. There is a 15% variation in the voltage values for data obtained in the absence of added nucleotide, and a 20% variation in the voltage values for data obtained in the presence of ADP at high temperature.

dependence on [DnaK] over a limited range of DnaK concentrations. For reactions conducted in the absence of nucleotide, the slope increased by a factor of 100 (40 to 4000 $M^{-1}s^{-1}$) between 25 and 42 °C. In contrast, for reactions conducted in the presence of Mg-ADP, the slope increased by a factor of 2 (1100 to 2400 M^{-1} s^{-1}) over the same temperature range. The linear dependence of k_d on [DnaK] is consistent with a bimolecular reaction as the cause of the loss of the DnaK−fVSV13 signal. A reasonable interpretation is that a DnaK−fVSV13 complex binds to a free monomer (E) or a free dimer (E_2) to yield an oligomeric DnaK−fVSV13 complex, with reduced fluorescence. Bound ADP modulates the kinetics of the reaction.

From experiments conducted under equilibrium conditions, it is known that peptide at large molar excesses shifts oligomeric states of 70-kDa chaperones to the monomeric state (Blond-Elguindi et al., 1993; Gao et al., 1996). Thus, if oligomerization was responsible for the reduction in the

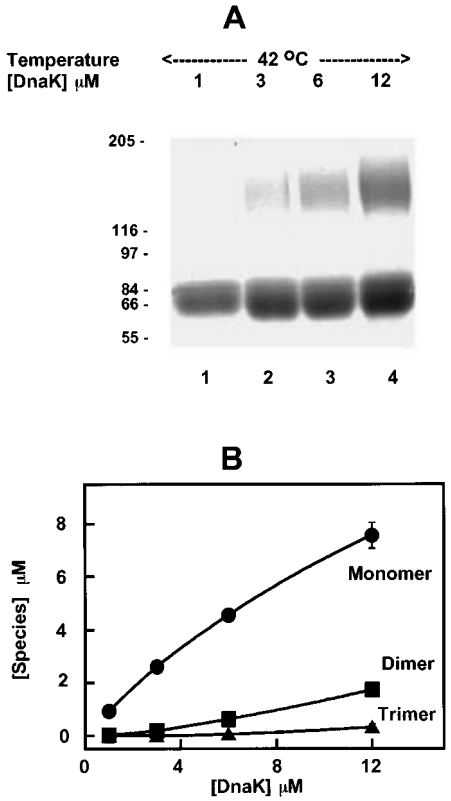

FIGURE 3: Concentration dependence of DnaK oligomerization at 42 °C. The cross-linking assay in conjunction with SDS−PAGE (3−7% polyacrylamide) was used to assess the effect of DnaK concentration on oligomerization at heat shock temperatures. (A) Cross-linking of DnaK was carried out according to the text (see Materials and Methods). Lane 1, 1.0 μM DnaK; lane 2, 3.0 μM; lane 3, 6.0 μM; and lane 4, 12 μM. The centers of mass of the two bands in lane 4 correspond to 140 kDa (dimer) and 70 kDa (monomer). (B) Plot of the concentration of DnaK monomers (●), dimers (■), and trimers (▲), derived from densitometric scans of the lanes in panel A. The concentration of the *i*th DnaK species is given by $[(I_i/n)/\sum_i I_i] \times$ [DnaK], where I_i is the intensity of a band on the gel, $\sum_i I_i$ is the sum of the intensities of the monomer, dimer, and trimer bands, n is the degree of oligomerization, and [DnaK] is the concentration of DnaK.

DnaK−fVSV13 signal in the biphasic traces, then excess fVSV13 should abolish the reduction because it inhibits oligomerization. This idea was tested by conducting pre-steady-state kinetic experiments in the presence of excess fVSV13 at 42 °C (data not shown). At a 3-fold molar excess of fVSV13 (18 μM) over DnaK (6 μM), after an initial burst in the DnaK−fVSV13 signal, there was a prominent descending phase in which approximately 50% of the signal was lost. In contrast, at a 10-fold molar excess of fVSV13 (60 μM) over DnaK (6 μM), the descending phase was absent. Our combined results show that both excess ATP and excess fVSV13 abolished the descending portion of the biphasic traces. Since both excess ATP and excess fVSV13 inhibit chaperone oligomerization, a reasonable conclusion is that the descending portion of the biphasic traces is a consequence of chaperone oligomerization.

Concentration Dependence of DnaK Oligomerization. To assess the concentrations of monomeric and oligomeric states of DnaK at 42 °C prior to mixing, DnaK samples were cross-linked with glutaraldehyde and then assayed via SDS−PAGE (Figure 3). These samples contained no nucleotide and no peptide. At 1.0 μM, DnaK was nearly 100% monomeric (lane 1). The most obvious change upon increasing the concentration of DnaK (1−12 μM) was the appearance of a dimer subpopulation (lanes 2−4). Note that the broad protein bands on the SDS−polyacrylamide gels (Figures 3 and 4) are due to intramolecular cross-linking, which tends to inhibit SDS loading. This effect has been observed in previous cross-linking studies of Hsc70 (Schlossman et al., 1984; Benaroudj et al., 1994). Each lane in Figure 3A was scanned with a densitometer to estimate the concentrations of monomeric, dimeric, and trimeric states of DnaK. The plot in Figure 3B shows a linear increase in the concentrations of all three chaperone species between 1 and 12 μM total DnaK. At every DnaK concentration, [monomers] >> [dimers] > [trimers].

Table 1: Effect of Nucleotide on DnaK Oligomerization

species	no nucleotide	+ADP	+ATP
	25 °C, [DnaK] = 6 μM		
monomer	85 ± 1	91 ± 1	99.5 ± 0.5
dimer	13 ± 1	10 ± 1	0.5 ± 0.5
trimer	2 ± 1	0	0
	42 °C, [DnaK] = 6 μM		
monomer	78 ± 2	90 ± 2	99.5 ± 1.5
dimer	20 ± 1	11 ± 2	0.5 ± 0.5
trimer	2 ± 2	0	0

[a] Mass percentages were determined by densitometric scans of the SDS gels. The mass percentage of the *i*th species is given by $M_i \times 100/\sum_i M_i$, where M_i and $\sum_i M_i$ are the mass of the *i*th species and the total mass, respectively.

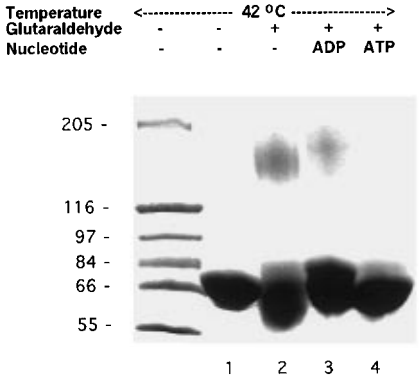

FIGURE 4: Effect of nucleotide on DnaK oligomerization at 42 °C. The cross-linking assay in conjunction with SDS−PAGE was used to assess the effect of nucleotide on DnaK oligomerization (see Materials and Methods). Lane 1, DnaK with no nucleotide and no cross-linking; lane 2, no nucleotide plus cross-linking; lane 3, Mg-ADP (2.0 mM) plus cross-linking; lane 4, Mg-ATP (2.0 mM) plus cross-linking. In each sample, [DnaK] = 6.0 μM. 6% polyacrylamide gel.

Experiments were designed to determine whether Mg-ATP shifts oligomers to monomers at heat shock temperatures. The results were compared to the effect of ATP on oligomerization at 25 °C. At 25 °C (data not shown), in the absence of nucleotide, the mass percentages of the DnaK species were 85% monomer, 13% dimer, and 2% trimer (Table 1). A sedimentation equilibrium analysis of DnaK at 25 °C gave similar results (Schönfeld et al., 1995). ATP completely inhibited oligomerization at 25 °C. At 42 °C, in the absence of glutaraldehyde, DnaK migrated as a single species, as expected (Figure 4, lane 1). When DnaK was cross-linked with glutaraldehyde in the absence of nucleotide, two bands appeared on the denaturing gel (lane 2), consistent with monomeric (78%) and dimeric (20%) DnaK. (A faint third band, consistent with the molecular weight of a DnaK

trimer, was also visible on the gel.) When DnaK was cross-linked in the presence of 2.0 mM ADP, two bands also appeared, consistent with monomeric (90%) and dimeric (11%) DnaK (lane 3). When DnaK was cross-linked in the presence of 2.0 mM ATP, a homogeneous population of monomeric DnaK was produced (lane 4). These cross-linking results show that at 25 and 42 °C ADP partially inhibits DnaK dimer formation, whereas ATP completely inhibits it.

We propose the following model to explain the kinetic and cross-linking results: (i) DnaK reversibly oligomerizes (reaction 1); (ii) upon mixing DnaK with labeled peptide, peptide binds to and induces a conformational change in the DnaK monomer which does not affect the fluorescence of the bound peptide (reaction 2); and (iii) the conformational change in the monomer promotes oligomer formation, which can quench the fluorescence of the bound peptide (reaction 3). Since DnaK monomers are the most abundant species, this oligomerization and quenching step probably corresponds to E + (EP)* ⇌ E-EP.

$$E \overset{[E]}{\rightleftharpoons} E_2 \overset{[E]}{\rightleftharpoons} E_3 \quad (1)$$

$$E + P \underset{k_{-1}}{\overset{k_1}{\rightleftharpoons}} (EP)^* \quad (2)$$

$$E_n + (EP)^* \underset{k_{-2}}{\overset{k_2}{\rightleftharpoons}} E_n{-}EP \ (n = 1 \text{ or } 2) \quad (3)$$

The term (EP)* denotes a monomeric DnaK−peptide complex in which the bound peptide is fluorescent, and E_n−EP denotes an oligomeric DnaK−peptide complex in which the fluorescence of the bound peptide is quenched. Because ATP maintains DnaK in a low-affinity, monomeric state, oligomerization and thus quenching are inhibited. In contrast, ADP only partially inhibits oligomerization. The effect of excess peptide on oligomerization is discussed below.

Least-Squares Fitting of the Stopped-Flow Data. The stopped-flow traces obtained in the absence of nucleotide (Figure 2A) were fitted to reactions 2 and 3 using the numerical integration and fitting program Scientist (see Materials and Methods). The following assumptions simplified the fitting: (i) The reversible reactions depicted in equilibrium 1 are slow (Schönfeld et al., 1995) compared to the time scale of peptide binding; therefore, the equilibrium was not included in the fitting. (ii) The maximum fluorescence ($F_{max} \sim 0.03$ V) in Figure 2 A corresponded to 50% of fVSV13 bound to DnaK ([DnaK−fVSV13] = 0.05 μM). (iii) The fluorescence values of free peptide P, monomer-bound peptide (EP)*, and bound but quenched peptide E_n·EP, were set equal to zero, one, and zero, respectively. (iv) Peptide does not bind directly to DnaK dimers or trimers.

The initial conditions were as follows. For a given concentration of DnaK, the data in Figure 3B were used to estimate the concentrations of monomers and dimers. For example, when [DnaK] = 5.6 μM, [E] = 4.4 μM and [E_2] = 0.6 μM; for [DnaK] = 4.6 μM, [E] = 3.8 μM and [E_2] = 0.4 μM; and for [DnaK] = 3.2 μM, [E] = 2.8 μM and [E_2] = 0.2 μM. In addition, at time zero, [P] = 0.1 μM and [(EP)*] = [E_n−EP] = 0. Initial guesses of the four rate constants (k_1, k_{-1}, k_2, k_{-2}) were made. Note that the initial guess for k_1 (2×10^5 M^{-1} s^{-1}) was obtained from the slope of a plot of k_{obs} versus [DnaK] (data not shown). These k_{obs} values were estimated by fitting the stopped-flow data in Figure 2A at early times to a single-exponential function. The above assumptions and initial conditions were used to fit stopped-flow data to reactions 2 and 3, as follows.

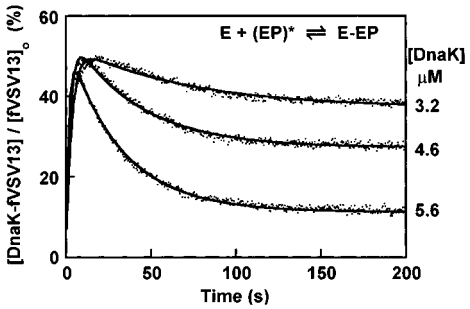

FIGURE 5: Numerical fitting of the stopped-flow data. Stopped-flow traces from Figure 2A were fitted to the differential equations associated with reactions 4 and 5 using the numerical integration program Scientist (see text). Calculated curves (solid lines) are superimposed on the stopped-flow traces. The calculated rate constants fall in the following ranges: $k_1 = (6-8) \times 10^4$ M^{-1} s^{-1}, $k_{-1} = (1-3) \times 10^{-1}$ s^{-1}, $k_2 = (4-9) \times 10^4$ M^{-1} s^{-1}, and $k_{-2} = (7-10) \times 10^{-3}$ s^{-1}. At time zero: [DnaK] = 5.6 μM, [E] = 4.4 μM; [DnaK] = 4.6 μM, [E] = 3.8 μM; and [DnaK] = 3.2 μM, [E] = 2.4 μM. [P] = 0.1 μM and [(EP)*] = [E−EP] = 0. The goodness of fit parameter R^2 was ~0.999 for each calculated trace shown above.

E + P ⇌ (EP); E + (EP)* ⇌ E−EP.* In this case, monomers bind peptide and participate in oligomerization; preexisting oligomeric states of DnaK were ignored. The resultant calculated traces are superimposed on the data in Figure 5. The calculated rate constants, for this case, are given in reactions 4 and 5.

$$E + P \underset{k_{-1} = (1.9 \pm 0.5) \times 10^{-1}\ s^{-1}}{\overset{k_1 = (6.4 \pm 0.8) \times 10^4\ M^{-1}\ s^{-1}}{\rightleftharpoons}} (EP)^* \quad (4)$$

$$E + (EP)^* \underset{k_{-2} = (9.5 \pm 2.0) \times 10^{-3}\ s^{-1}}{\overset{k_2 = (6.7 \pm 2.9) \times 10^3\ M^{-1}\ s^{-1}}{\rightleftharpoons}} E{-}EP \quad (5)$$

E+P ⇌ (EP); E_2 + (EP)* ⇌ E_2−EP.* Although [monomers] >> [dimers], we nevertheless fitted the stopped-flow data to reactions 2 and 3 with the stipulation that monomers bind peptide and dimers bind monomeric DnaK−peptide complexes. The resultant calculated traces were identical to those shown in Figure 5 (data not shown). The calculated rate constants, for this case, are given in reactions 6 and 7.

$$E + P \underset{k_{-1} = (1.9 \pm 0.5) \times 10^{-1}\ s^{-1}}{\overset{k_1 = (6.3 \pm 0.8) \times 10^4\ M^{-1}\ s^{-1}}{\rightleftharpoons}} (EP)^* \quad (6)$$

$$E_2 + (EP)^* \underset{k_{-2} = (8.6 \pm 1.6) \times 10^{-3}\ s^{-1}}{\overset{k_2 = (6.4 \pm 1.5) \times 10^4\ M^{-1}\ s^{-1}}{\rightleftharpoons}} E_2{-}EP \quad (7)$$

The above fitting procedures yielded nearly identical values for the "on" and "off" rate constants for fVSV13 binding to and dissociating from DnaK ($k_1 = 6.4 \times 10^4$ M^{-1} s^{-1} and $k_{-1} = 1.9 \times 10^{-1}$ s^{-1}). Using these rate constants, an equilibrium dissociation constant (K_d) for the dissociation of fVSV13 from DnaK was calculated: $K_d = k_{-1}/k_1 = 1.9 \times 10^{-1}$ $s^{-1}/6.3 \times 10^4$ M^{-1} $s^{-1} = 3 \times 10^{-6}$ M (at 42 °C). For this same reaction, an equilibrium dialysis study showed that $K_d = 2.6 \times 10^{-6}$ M (at 25 °C) (Buchberger et al., 1994). On the basis of these numerical fittings, we conclude that DnaK monomers or DnaK dimers, or probably both, can participate in the proposed oligomerization reaction.

An attempt was also made to fit the stopped-flow data to the two-step sequential reaction $E + P \rightleftharpoons EP^* \rightleftharpoons EP$. The first step ($E + P \rightleftharpoons EP^*$) corresponds to the binding of a labeled peptide to the chaperone monomer to yield a fluorescent chaperone−peptide complex. The second step ($EP^* \rightleftharpoons EP$) corresponds to a conformational change in the chaperone or the peptide or both, which leads to the quenching of the fluorescence of the bound peptide. The data could not be fitted to this two-step sequential reaction.

DISCUSSION

The results in this report are consistent with a mechanism involving peptide-induced oligomerization of DnaK as an explanation of the biphasic stopped-flow data. Our proposed kinetic model postulates that peptide binding to a chaperone monomer induces a conformational change in the monomer which can lead to oligomerization at sufficiently high chaperone concentrations (reactions 1−3). Note that DnaK is one of the most abundant *E. coli* proteins, and when the temperature is increased from 15 to 46 °C, there is a 4-fold increase in its concentration (Herendeen et al., 1979). Several studies have shown that peptide binding induces a conformational change in the chaperone monomer (Flynn et al., 1989; Park et al., 1993; Fung et al., 1996). Another way to envision this peptide-induced conformational change is that when peptide binds to a chaperone monomer a cryptic binding site is exposed. This idea is supported by recent reports that DnaK may have two peptide binding sites: one site for hydrophilic substrates, the other for hydrophobic substrates (Takenaka et al., 1995; deCrouy-Chanel et al., 1996). In a related study, it was shown that when a hydrophilic substrate binds to a molecule of the *E. coli* chaperone SecB, a cryptic, hydrophobic binding site is exposed (Randall, 1992). We suggest that the binding of fVSV13 to DnaK in the absence of nucleotide or with ADP exposes a hydrophobic binding site, and at sufficiently large concentrations of DnaK, monomers or dimers bind to the monomeric DnaK−peptide complex to form oligomeric DnaK−peptide complexes.[2] There are several reports of oligomeric states of 70-kDa chaperones with bound (poly)-peptides. For example, a BiP dimer with a bound peptide has been reported by two different groups (Blond-Elguindi et al., 1993; Brot et al., 1994), and complexes between λP, a protein involved in bacteriophage λ replication, and dimeric and trimeric DnaK have been reported (Osipiuk et al., 1993).

Large concentrations of the fVSV13 peptide abolished the descending portion of the biphasic traces. A reasonable interpretation of this result is that peptide at large concentrations saturates all of the available peptide binding sites and thereby inhibits oligomerization and quenching (reaction 3). Even if only dimers participate in the oligomerization and quenching reaction, large concentrations of peptide can either shift the monomer−dimer equilibrium to the monomer state via binding to monomers (Gao et al., 1996) or disrupt dimers to monomers via direct binding to dimers (Blond-Elguindi et al., 1993). Especially in the latter case, large concentrations of peptide might be necessary if dimers have a low affinity for peptide. The liberated monomers bind peptide and are therefore unable to interact with other monomeric DnaK−peptide complexes.

It is useful to compare features of the stopped-flow traces acquired at 25 °C and 42 °C at 6 μM DnaK (Figures 1 and 2A). Although the DnaK−fVSV13 signal was always about 2.5 times greater at 25 °C ($F_{max} = 0.070$ V) than at 42 °C ($F_{max} = 0.028$ V), the respective reductions in the signals (ΔF) were similar: $\Delta F = 0.016$ and 0.020 V at 25 °C and 42 °C. The main difference between these two traces was that the *rate* of the reduction in the DnaK−fVSV13 signal was much slower at 25 °C than at 42 °C. We interpret this phenomenon as the chemical reaction that causes the fluorescence quenching in the absence of nucleotide having a large activation energy barrier. This is plausible since the slope of the plot of k_d versus [DnaK], which is a composite constant made up of the four individual rate constant (k_1, k_{-1}, k_2, and k_{-2}), increased a 100-fold (from 40−4000 M^{-1} s^{-1}) when the temperature was raised only 17 °C (Figure 2B).

Although the proposed model (reactions 1−3) does not explicitly depict states of DnaK with bound ADP, it precisely accounts for the kinetic results obtained in the presence of ADP. In other words, bound ADP may alter one or more of the reaction rates, but does not alter the mechanism. One way to test this proposed model is to conduct kinetic experiments using a genetically engineered form of DnaK which does not oligomerize.

[2] Using high-performance size-exclusion chromatography with fluorescence and absorbance detection, we have detected the fVSV13 peptide bound to both DnaK monomers and dimers (Farr and Witt, unpublished results).

ACKNOWLEDGMENT

We thank Drs. Robert Rhoads and Robert Smith for critical reading of the manuscript and for excellent suggestions.

REFERENCES

Becker, G., & Craig, E. A. (1994) *Eur. J. Biochem. 219*, 11−23.
Benaroudj, N., Fang, B., Triniolles, F., Ghelis, C., & Ladjimi, M. M. (1994) *Eur. J. Biochem. 221*, 121−128.
Benaroudj, N., Batelier, G., Triniolles, F., & Ladjimi, M. M. (1995) *Biochemistry 34*, 15282−15290.
Bevington, P. R. (1969) in *Data Reduction and Error Analysis for the Physical Sciences*, pp 237−240, McGraw-Hill, New York.
Blond-Elguindi, S., Fourie, A. M., Sambrook, J. F., & Gething, M.-J. H. (1993) *J. Biol. Chem. 268*, 12730−12735.
Brot, N., Redfield, B., Qiu, N.-H., Chen, G.-J., Vidal, V., Carlino, A., & Weissbach, H. (1994) *Proc. Natl. Acad. Sci. U.S.A. 91*, 12120−12124.
Buchberger, A., Valencia, A., McMacken, R., Sander, C., & Bukau, B. (1994) *EMBO J. 13*, 1687−1695.
Carlino, A., Toledo, H., Skaleris, D., DeLisio, R., Weissbach, H., & Brot, N. (1992) *Proc. Natl. Acad. Sci. U.S.A. 89*, 2081−2085.
Chaykin, S. (1966) in *Biochemistry Laboratory Techniques*, pp 137, John Wiley & Sons, Inc., New York.
deCrouy-Chanel, A., Kohiyama, M., & Richarme, G. (1996) *J. Biol. Chem. 271*, 15486−15490.
Farr, C. D., Galiano, F. J., & Witt, S. N. (1995) *Biochemistry 34*, 15574−15582.
Flaherty, K. M., DeLuca-Flaherty, C., & McKay, D. B. (1990) *Nature 346*, 623−628.
Flaherty, K. M., McKay, D. B., Kabsch, W., & Holmes, K. C. (1991) *Proc. Natl. Acad. Sci. U.S.A. 88*, 5041−5045.
Flynn, G. C., Chappell, T. G., & Rothman, J. E. (1989) *Science 245*, 385−390.
Fourie, A. M., Sambrook, J. F., & Gething, M.-J. H. (1994) *J. Biol. Chem. 269*, 30470−30478.
Fung, K. L., Hilgenberg, L., Wang, N. M., & Chirico, W. J. (1996) *J. Biol. Chem. 271*, 21559−21565.
Gallione, C. J., & Rose, J. K. (1983) *J. Virol. 46*, 162−169.
Gao, B., Eisenberg, E., & Greene, L. (1996) *J. Biol. Chem. 271*, 16792−16797.

Georgopoulos, C., & Welch, W. J. (1993) *Annu. Rev. Cell Biol. 9*, 601−634.
Ha, J.-H., & McKay, D. B. (1995) *Biochemistry 34*, 11635−11644.
Hames, B. D., & Rickwood, D. (1990) in *Gel Electrophoresis of Proteins. A Practical Approach* (Rickwood, D., & Hames, B. D., Eds.) pp 44−46, IRL Press at Oxford University Press, New York.
Hendrick, J. P., & Hartl, F.-U. (1993) *Annu. Rev. Biochem. 62*, 349−384.
Herendeen, S. L., VanBogelen, R. A., & Neidhardt, F. C. (1979) *J. Bacteriol. 139*, 186−194.
Laemmli, U. K. (1970) *Nature 227*, 680−685.
Montgomery, D., Jordan, R., McMacken, R., & Freire, E. (1993) *J. Mol. Biol. 232*, 680−692.
Osipiuk, J., Georgopoulos, C., & Zylicz, M. (1993) *J. Biol. Chem. 268*, 4821−4827.
Palleros, D. R., Reid, K. L., Shi, L., & Fink, A. L. (1993a) *FEBS Lett. 336*, 124−128.
Palleros, D. R., Reid, K. L., Shi, L., Welch, W. J., & Fink, A. L. (1993b) *Nature 365*, 664−666.
Park, K., Flynn, G. C., Rothman, J. E., & Fasman, G. D. (1993) *Protein Sci. 2*, 325−330.
Randall, L. L. (1992) *Science 257*, 241−245.
Sadis, S., & Hightower, L. E. (1992) *Biochemistry 31*, 9406−9412.
Schlossman, D. M., Schmid, S. L., Braell, W. A., & Rothman, J. E. (1984) *J. Cell Biol. 99*, 723−733.
Schmid, S. L., Braell, W. A., & Rothman, J. E. (1985) *J. Biol. Chem. 260*, 10057−10062.
Schönfeld, H.-J., Schmidt, D., Schröder, H., & Bukau, B. (1995) *J. Biol. Chem. 270*, 2183−2189.
Shi, L., Kataoka, M., & Fink, A. L. (1996) *Biochemistry 35*, 3297−3308.
Takenaka, I. M., Leung, S.-M., McAndrew, S. J., Brown, J. P., & Hightower, L. W. (1995) *J. Biol. Chem. 270*, 19838−19844.
Toledo, H., Carlino, A., Vidal, V., Redfield, B., Nettleton, M. Y., Kochan, J. P., Brot, N., & Weissbach, H. (1993) *Proc. Natl. Acad. Sci. U.S.A. 90*, 2505−2508.
Zhu, X., Zhao, X., Burkholder, W. F., Gragerov, A., Ogata, C. M., Gottesman, M. E., & Hendrickson, W. A. (1996) *Science 272*, 1606−1614.
Zylicz, M., & Georgopoulos, C. (1984) *J. Biol. Chem. 259*, 8820−8825.

BI971082F